Synthesis and Characterization of Photo-Cross-Linkable Hole-Conducting Polymers

Erwin Bacher,[†] Michael Bayerl,[†] Paula Rudati,[‡] Nina Reckefuss,[‡] C. David Müller,[‡] Klaus Meerholz,[‡] and Oskar Nuyken*,[†]

Lehrstuhl für Makromolekulare Stoffe, Technische Universität München, Lichtenbergstrasse 4, D-85747 Garching, Germany, and Institut für Physikalische Chemie, Universität Köln, Luxemburgerstrasse 116, D-50939 Cologne, Germany

Received August 9, 2004; Revised Manuscript Received November 29, 2004

ABSTRACT: The synthesis and characterization of side-chain polymers functionalized with hole-transporting units and photo-cross-linkable groups, which can be used for solution-based preparation of multilayer organic light-emitting devices (OLEDs), are discussed. The concept deals with triarylamine and oxetane-functionalized styrenes, which are copolymerized by radical polymerization. Four different types of hole-transporting monomers were combined with one cross-linkable monomer in two different ratios, yielding two groups of each four polymers (**P1A**...**P4A** and **P1B**...**P4B**). The polymers were investigated by NMR spectroscopy, molecular weights were determined by GPC with light scattering, and the thermal properties were measured with differential scanning calorimetry (DSC). Optical characterization by UV−vis and fluorescence spectroscopy was performed. Electrochemical and cross-linking characteristics of the copolymers were investigated to proove this strategy's potential in application for modern multilayer polymer OLEDs. Finally, hole-only devices were prepared for evaluation of the semiconductive performance of the materials.

Introduction

Modern organic light-emitting diodes (OLEDs) consist of two or more different layers[1] to enhance electro-optical properties and stability. During processing of the devices via layer-by-layer coating, the subsequent layer has to be coated onto the previous layer without altering it. A useful method to avoid redissolution is to cross-link the coated layer before applying the next one.[2] Cross-linked polymers are used in manifold ways for OLEDs.[3−6] Photo-cross-linking became an especially common strategy of protecting polymer films against solvents.[7−9] Generally, for the preparation of OLEDs, a precursor consisting of charge-transporting or emitting groups and pendant photo-cross-linkable function is dissolved in a suitable solvent. A certain amount of photoinitiator is added before this solution is spin-coated onto a substrate. Then, the layer is dried and finally cross-linked by irradiation with UV light. After this step, the next layer can be produced the same way on top of the first one without altering the original layer and so on.

For achieving homogeneous and crack-free layers, the polymerizable group used for this cross-linking should show only little volume shrinkage, short conversion time, and nearly quantitative yield. The oxetane unit, which fulfills the requirements almost ideally, is used in our work as a pendant cross-linkable group.[10] It shows an ideal combination of cross-linkability on one hand and processability on the other hand. Furthermore, it is inert to coupling conditions so that convergent synthesis can be carried out. A significant advantage of this photopolymerization-based process is the absence of any small molecules after cross-linking, caused by polycondensation reactions, which were also used for generating stable films.[24]

Several strategies are applied in our workgroup to combine emitting or charge-transporting properties with cross-linkability: first, cross-linker functionalized low-molecular-weight charge-transport molecules,[11] second, polymers with emitter or charge transporter as a part of the backbone are used.[12] In this paper, we propose side-chain-functionalized inert polymer backbones, e.g., poly(styrene)s with pendant emitter or charge transporter. In all cases, the cross-linkable groups are placed in the side chain. The synthesis and characterization of such copolymers, made from cross-linker- and charge-transporter-functionalized monomers, are described in some detail.

Results and Discussion

Monomer Synthesis. Copolymerization of both hole-conductor- and oxetane-functionalized styrene yields polymers with pendant charge-transporting and cross-linkable oxetane units. Advantages of this strategy are the freedom to choose the polymer, no residues of a polymerization catalyst, and due to the broad variety of functionalized monomers, the synthesis of tailor-made hole-conducting polymers. The different monomer structures, which have their own individual oxidation potentials, form a "construction kit" which allows for the synthesis of an optimized polymer for the corresponding application. However, the dilution of the active functions by the inert polymer backbone, spacer, and cross-linking groups should be considered as a possible disadvantage leading to reduced conductivity.

The electrochemical potential of charge transporters has to be adapted to the electrode work function and to the HOMO of the adjacent emitting layer. Variations of the triarylamine unit allow for fine-tuning of the redox properties of the hole-transporting layer. The same cross-linking monomer was applied in each case.

* Author to whom correspondence should be addressed. Phone: +498928913571. Fax: +498928913562. E-mail: oskar.nuyken@ch.tum.de.
[†] Technische Universität München.
[‡] Universität Köln.

10.1021/ma048365h CCC: $30.25
Published on Web 02/08/2005

Scheme 1. Synthesis of Oxetane-Functionalized Monomer C1

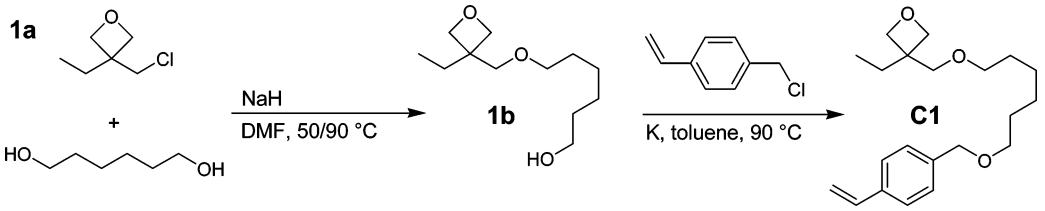

Scheme 2. Synthetic Pathways to Hole-Conducting Monomers H1−H4

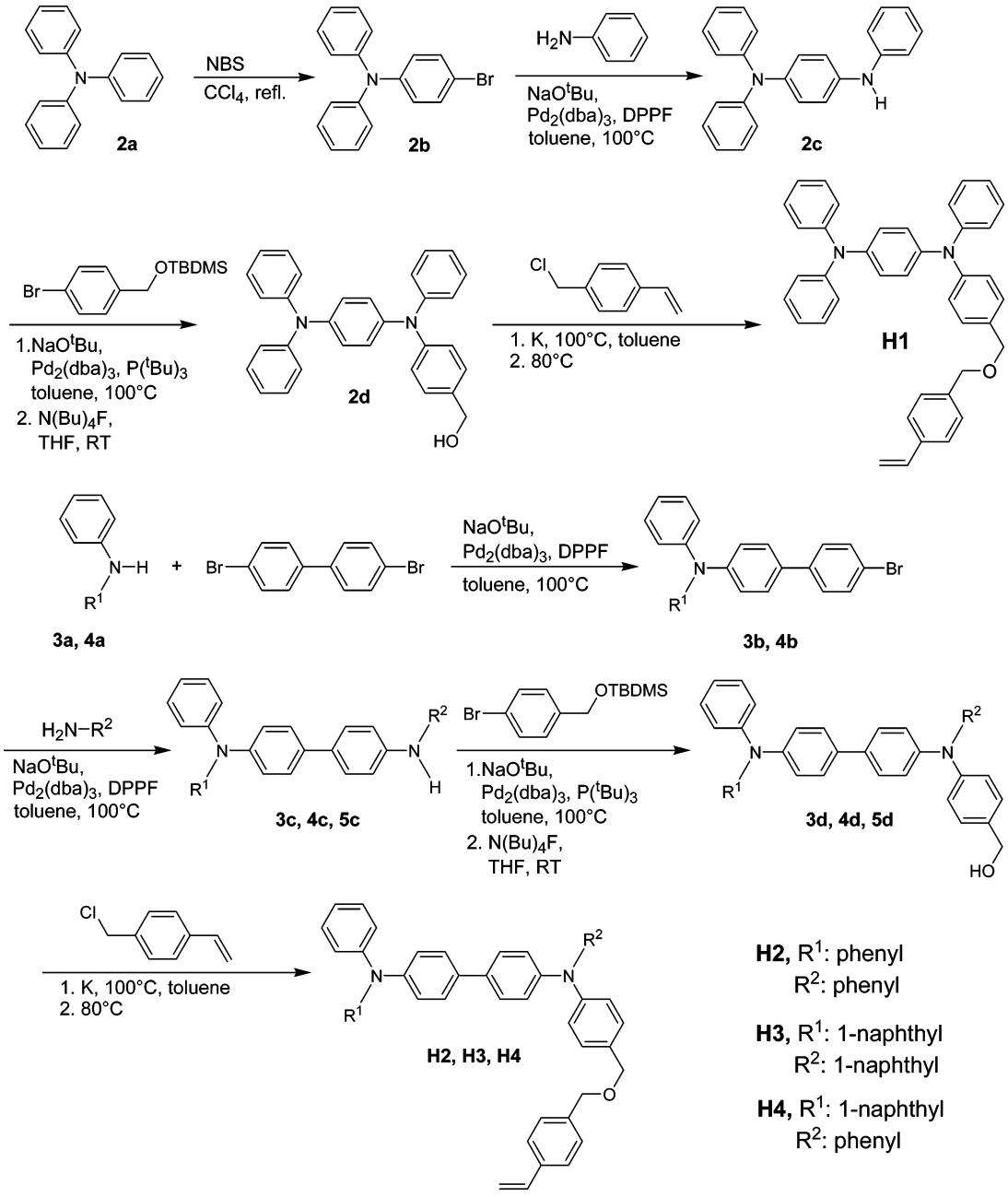

Earlier work showed that the cross-linking is improved by using a relatively long alkyl spacer between the functional unit and the oxetane unit, ultimately giving sufficient diffusional mobility to the oxetanes to react.[13] We found that hexyl spacers gave excellent results.

The oxetane-functionalized monomer **C1** was synthesized by a two-step etherification. First, 3-chloromethyl-3-ethyl oxetane **1a**[14,15] was reacted with 1,6-hexanediol yielding **1b**, and then the resulting product was coupled with 4-vinyl benzyl chloride, yielding the desired product **C1** (Scheme 1). A common C−N coupling route, the Hartwig−Buchwald amination, is used for the synthesis of hole-conducting monomers (Scheme 2).[16−18] Synthesis of **H1** starts with the bromination of triphenylamine by *N*-bromosuccinimide (NBS), which is highly regioselective, yielding **2b**. After two C−N coupling steps, first with aniline (**2b** → **2c**) and second with protected 4-bromobenzyl alcohol, a hydroxymethyl-substituted tetraphenyl phenylenediamine was obtained after depro-

Scheme 3. Copolymerization of Styrene-Functionalized Hole Conductor H1−H4 and Cross-Linker C1, Leading to Polymers P1A/B−P4A/B

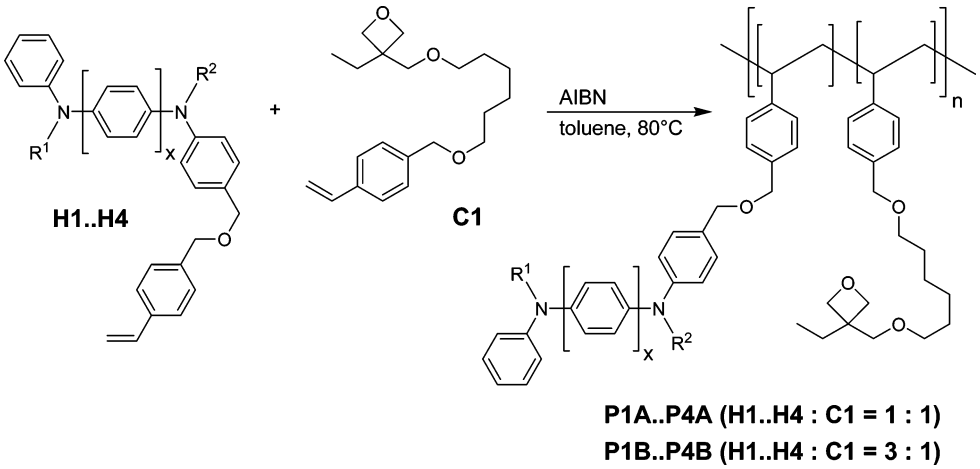

Table 1. Data for P1A/B−P4A/B

	P1A	P1B	P2A	P2B	P3A	P3B	P4A	P4B
M_n (10^4 g/mole)	11.1	10.7	11.3	7.6	9.5	8.8	14.6	12.2
M_w/M_n	1.92	2.30	2.26	2.39	2.31	2.08	2.18	1.82
λ_{max} (nm) absorption	320		360		345		350	
λ_{max} (nm) fluorescence	406		422		457		444	
yield (%)	85	88	92	95	90	95	85	87
N content (%) calcd	3.1	4.2	2.9	3.8	2.6	3.3	2.8	3.5
found	3.1	4.1	2.9	3.8	2.6	3.1	2.7	3.5
T_g (°C)	54	74	67	83	72	86	70	84
molar ratio H/C[a]	0.98/1	2.89/1	1.08/1	3.05/1	1.08/1	3.11/1	1.05/1	3.10/1

[a] Calculated from the ratio between ^{1}H NMR Integrals of the oxymethylene groups of cross-linker (δ = 3.4) and all oxymethylene groups (δ = 3.4 and 4.4)

tection of the OH group (**2c** → **2d**). Etherification of **2d** with 4-vinylbenzyl chloride yields **H1**.

The monomers **H2**, **H3**, and **H4** were synthesized starting from the corresponding secondary amines **3a** and **4a**, which were coupled with 4,4′-dibromobiphenyl yielding **3b** and **4b**. A sequence of two further coupling steps, first with primary aromatic amines, yielding **3c**, **4c**, and **5c** and second between the secondary amines and protected 4-bromobenzyl alcohol, followed by a deprotection step yields **3d**, **4d**, and **5d**. Finally, **H2**, **H3**, and **H4** were obtained by introducing the unsaturated carbon function via etherification with 4-vinylbenzyl chloride.

Polymer Synthesis and Characterization. Copolymers of styrene-functionalized hole transporters (**H1**, **H2**, **H3**, **H4**) and a styrene-functionalized oxetane (**C1**) were synthesized by standard free-radical solution polymerization methods with AIBN as initiator (Scheme 3). Copolymers with two different monomer ratios were synthesized in order to investigate the influence of oxetane content on cross-linking properties on one hand and charge transporting performance on the other hand. Polymers (**P1B**−**P4B**) with a molar ratio **H1**(or **H2**, **H3**, **H4**)/**C1** = 3:1 seem to be good hole transporters but may show incomplete cross-linking, whereas polymers (**P1A**−**P4A**) with the ratio 1:1 show complete cross-linking but may have weaker charge-transporting properties.

Molecular weights and polydispersity indices (PDIs) of the polymers were determined by gel permeation chromatography (GPC) with a light scattering (LS) detector at λ = 690 nm, using chloroform as solvent (Table 1). UV−vis absorption and fluorescence spectra were recorded to evaluate the optical properties of the copolymers. Due to their higher contents of hole-transporting groups, **P1B**−**P4B** show increased absorption compared to their analogues **P1A**−**P2A** but show the same shape of the curve. The ratio between the absorption intensities of both types of polymers corresponds to the expected ratio, which results from the different monomer feed ratios. Furthermore, the nitrogen content was determined to verify the copolymerization ratios, and the values are in accordance with the calculated contents and calculated from the ratio between ^{1}H NMR integrals of the oxymethylene groups of cross-linker (δ = 3.4) and all oxymethylene groups (δ = 3.4 and 4.4)

The mobility of the oxetane groups is important to achieve complete cross-linking of the polymer layers. As a consequence, the polymers should show a glass transition temperature (T_g) below the curing temperature of the film after UV irradiation. The T_g's were measured by differential scanning calorimetry (DSC). All polymers show a T_g below the used minimum curing temperature of 100 °C.

The free-radical polymerization process leads to a relatively broad molecular-weight distribution of the polymers (PDI > 2). Regarding the potential application, this does not constitute a disadvantage since the polymer layer is cross-linked after application onto a substrate anyway. Nevertheless, the molecular weight must be sufficiently high to enable sufficient film-forming capabilities and to ensure that every polymer chain bears at least two oxetane units which participates in the cross-linking process. For a molecular weight of 10.000 g/mol, each chain contains on average about 8−9 oxetane units.

Cross-Linking. Cross-linking of films of **P1**−**P4** proceeds via cationic polymerization, which is commonly used for oxetanes.[19,20] The commercially available photoinitiator **6** (**PI**; Scheme 4) was added to initiate the

Scheme 4. Chemical Structures of the Low-Molecular-Weight Hole Conductor OTPD[22,23] Used as Reference Material and Iodonium Photoinitiator 6 (PI)

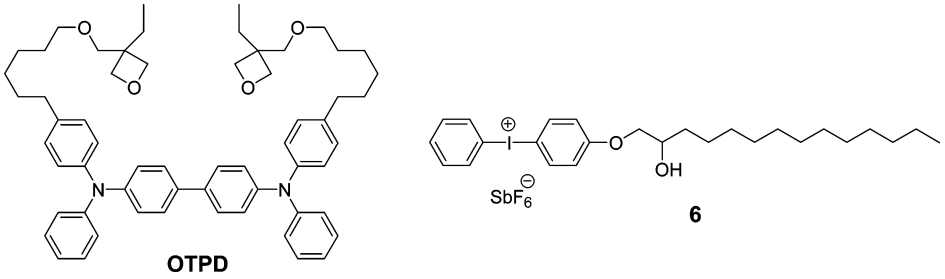

cross-linking process. During ultraviolet (UV) illumination, this photoacid decomposes via a multiple-step mechanism and generates protons, which open the oxetane ring and start the polymerization. First, we investigated the optimal conditions for cross-linking in order to obtain complete solvent resistivity (SR; see Experimental Section for details). We found that for PI contents below 5 wt% complete SR could not be achieved at room temperature. This is attributed to the fact that the viscosity of a film increases dramatically during the polymerization, such that the diffusional motion of the oxetane units is strongly hindered. Thus, the reaction stops for mechanical reasons; however, the chain ends (carbocations) are still intact. Under these conditions, however, the films are often still partly soluble. Curing at an elevated temperature softens the films such that the cross-linking reaction can proceed further, leading in the ideal case to complete insolubility. The progress of cross-linking was also studied by Fourier transform infrared (FTIR) spectroscopy.

Figure 2 shows the SR of 100 nm thick film of the polymers **P3A** and **P3B** with different ratios of the hole-transport monomer and the cross-linkable monomer. Similar results were obtained for the other three polymers. The dependence on the PI content for constant curing temperature (here, $T = 100$ °C) clearly shows that the SR increases as the PI content increases and then levels for c(PI) > 2 wt%, i.e., increasing the PI content beyond this does not lead to an improved SR. Furthermore, it is obvious that the polymer **P3A** is more easily cross-linked than **P3B**, which is expected due to the higher density of oxetane units.

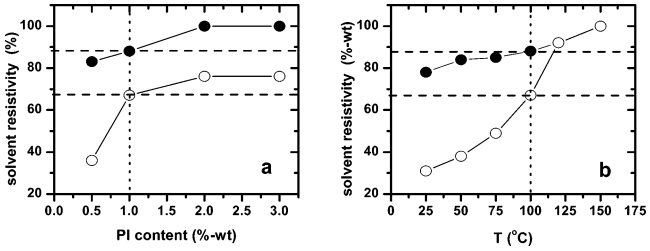

Figure 1. Dependence of the solvent resistivity (SR) of the polymers **P3A** (solid circles) and **P3B** (open circles) on the PI content at a curing temperature of 100 °C (a) and the curing temperature, T, at PI = 1 wt% (b). The lines are guides to the eye.

When the curing temperature is varied for a constant PI content (here, 1 wt%) we found a higher curing temperature led to significantly improved SR. The lower the curing temperature, the larger the difference in SR between the two types of polymers. The gap becomes smaller, and ultimately for the highest curing temperatures (T > 150 °C), SR = 100% could be achieved in all cases.

Electrochemical Characterization. The redox chemical properties of the cross-linked films were investigated by cyclic voltammetry. In analogy to low-molecular-weight triarylamines,[21] it was possible to reversibly convert the triarylamine groups of the polymers first to a radical cation then to a dication in all four cases. A typical example is shown in Figure 3 for the polymer **P3A**; we found no changes in electrical performance of the material during 10 cycles, an important prerequisite for application as hole conductor in OLEDs. Table 2 lists the oxidation potentials for **P1**−**P4**. In each case, the identical potentials were obtained for the A- and the B-series, respectively.

It is worth mentioning that the cationic form of the hole-transport polymer is soluble in acetonitrile; therefore, film degradation of the un-cross-linked polymer takes place which can also be recognized in a weak reduction curve. This drawback can be avoided com-

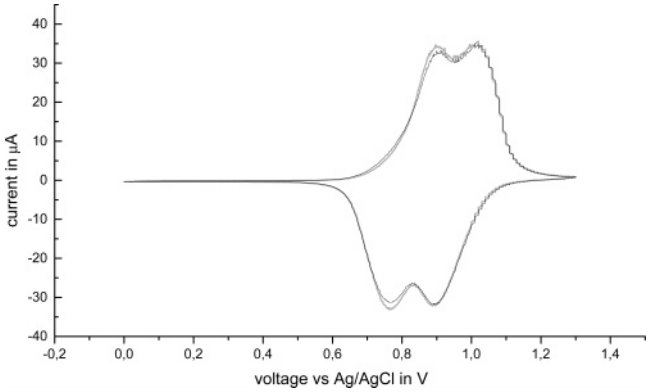

Figure 2. Cyclic voltammograms of a cross-linked film of **P3A** in a 0.05 M solution of Bu_4NPF_6 in acetonitrile. We show the first and the tenth cycle.

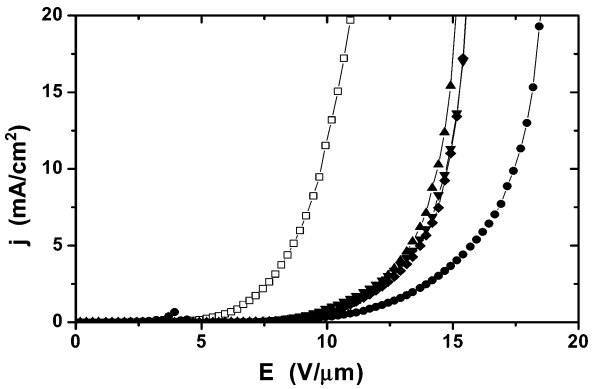

Figure 3. Field dependence of the current in hole-only devices ITO/**PnA**/Ag (150 nm) made of OTPD (squares) **P1A** (circles), **P2A** (up triangles), **P3A** (down triangles), and **P4A** (diamonds). The initiator concentration was 1 wt%; curing was performed at 150 °C for 60 s. The lines are guides to the eye.

Table 2. Redox Potentials of P1−P4 Relative to Ferrocene

	P1	P2	P3	P4
potential for P/P^+ (mV)	241	455	490	479
potential for P^+/P^{2+} (mV)	643	553	610	584

pletely by cross-linking the polymer before the electrochemical experiments (see Experimental Section). After cross-linking, the films are perfectly stable during cyclovoltammetry.

The differences in the redox potentials for the four transport units is in perfect agreement with the low-molecular-weight analogues. The first oxidation **P1/P1**$^{+\bullet}$ takes place at a low potential compared to **P2/P2**$^{+\bullet}$, whereas the potential of the second oxidation **P1**$^{+\bullet}$**/P1**$^{2+}$ is higher compared to **P2**$^{+\bullet}$**/P2**$^{2+}$. This is due to different electronic coupling between the charge-bearing subunits (N atoms); the reduction of the intramolecular distance (biphenyl (**P2**) → benzene (**P1**)) leads to a higher splitting of the half-wave oxidation potentials.[21] The naphthyl group lowers the electron density at the nitrogen compared to phenyl; therefore, oxidation of **P3** is only possible at higher potentials compared to those of **P2**. The values for **P4** lie between **P2** and **P3** as expected.

Hole-Only Devices. Hole-only devices were prepared to characterize the transport properties of the novel polymers. The current−voltage diagrams are shown in Figure 3. All polymers show significantly higher onset voltages than the low-molecular-weight reference **OTPD**. One possible explanation for this finding could be differences in the ratio between active (i.e., hole conductive) and inactive (alkyl spacers and oxetane) units. In the 1:1 polymers (A-series), the inactive units account for about 35% of the repeat unit, while in **OTPD**, about 25% of the molar mass is inactive. Additionally, the relative orientation of the triarylamine units might be more favorable in **OTPD**.

Conclusion

In conclusion, a variety of cross-linkable polymers suitable as hole transporters were synthesized and characterized. The cross-linked films show high mechanical stability, as well as fully reversible electrochemical characteristics. Concerning the cross-linkability and oxidation potentials, these polymers meet the requirements of a hole-transport layer in OLEDs. Hole-only devices made from the novel materials exhibited higher onset voltages than low-molecular-weight cross-linkable analogues. The concept of styrene-based functional materials is very versatile and allows us to synthesize other polymers with optimized hole conductor/cross-linker ratios for optimization of onset voltage.

Experimental Section

General Details. All synthesis steps were carried out under nitrogen using standard Schlenk techniques. Toluene, diethyl ether, and tetrahydrofuran were distilled from sodium under nitrogen. Cyclohexane, toluene, and ethyl acetate for column chromatography were distilled from technical grade solvents and recycled after use. All other chemicals were reagent grade and used as received (ABCR, Aldrich, Merck, Strem) without further purification. If necessary, the products were purified by column chromatography with silica gel (Fluka, KG 60, 0.063−0.2 mm).

Gel permeation chromatography (GPC) with light-scattering detection was carried out using a Styragel HR 4E column, a 2414 differential refractometer, a 484 UV detector (all from Waters), and a Wyatt miniDAWN light-scattering detector (λ = 690 nm) on samples in $CHCl_3$. All samples were filtered through a 0.22 μm Teflon filter (Millipore) to remove solid particles. UV−vis spectra were recorded on a Varian Cary 3 spectrophotometer in the range 280−500 nm. Elemental analyses (C, H, N) were performed on a Elementar Vario EL analyzer. NMR data were obtained on a Bruker ARX 300 at 300.13 MHz (^{1}H) and 75.48 MHz (^{13}C) and are listed in parts per million (ppm) downfield from tetramethylsilane for proton and carbon. Abbreviations for aromatic C and H atoms are: bz = benzyl, dphe = diphenylene, mph = 4-methylphenyl, na = 1-naphthyl, ox = oxetane, ph = phenyl, phe = phenylene, and vbz = 4-vinylbenzyl; o, m, and p stand for ortho, meta, and para relative to N or Br atoms. Coupling constants are given in Hertz (Hz). FT-IR spectra (ATR spectra and KBr spectra) were recorded on a Bruker IFS 55 spectrophotometer. EI mass spectra were recorded by a Finnigan MAT 8200 mass spectrometer. The monomers were dissolved in benzene for the freeze-drying procedure. The resulting solution was frozen with liquid nitrogen and then allowed to slowly reach room temperature in a vacuum.

3-Ethyl-3-(6-hydroxyhexyl)oxymethyl-oxetane 1b. Sodium hydride (2.88 g, 120 mmol) was suspended in 200 mL of dimethylformamide (DMF) under N_2 atmosphere. 1,6-Hexanediol (47.3 g, 400 mmol), dissolved in 200 mL of DMF, was added to the suspension. After being degassed and saturated with N_2, the mixture was stirred at 50 °C until the H_2 evolution had ceased (ca. 1 h). 3-Chloromethyl-3-ethyloxetane **1a** (13.5 g, 100 mmol) was added, and the mixture was stirred at 90 °C for 16 h. After being cooled to room temperature, the solvent was removed in a vacuum, the residue was dissolved in 300 mL of diethyl ether and was washed three times with 200 mL of water. The organic layer was dried over $MgSO_4$, and the solvent was evaporated. The crude product was purified by distillation in a glass oven at 170−180 °C/0.3 hPa to give a clear, colorless liquid (13.2 g, 61%). $C_{12}H_{24}O_3$ (216.32 g/mol). Anal. Calcd (%): C, 66.63; H, 11.18. Found (%): C, 65.23; H, 10.89. ^{1}H NMR ($CDCl_3$) δ: 4.38 (d, 2H, $^2J_{H,H}$ = 5.73 Hz, H-ox); 4.30 (d, 2H, $^2J_{H,H}$ = 5.73 Hz, H-ox); 3.57 (t, 2H, $^3J_{H,H}$ = 6.30 Hz, −CH_2−O−); 3.45 (s, 2H, −O−CH_2−); 3.39 (t, 2H, $^3J_{H,H}$ = 6.51 Hz, −CH_2−OH); 1.67 (q, 2H, $^3J_{H,H}$ = 7.62 Hz, H_3C−CH_2−); 1.51 (m, 4H, −CH_2−); 1.32 (m, 4H, −CH_2−); 0.82 (t, 3H, $^3J_{H,H}$ = 7.44 Hz, −CH_3). ^{13}C NMR ($CDCl_3$) δ: 78.9 (−*C*H_2−, ox); 73.8 (-*C*H_2−O-); 71.9 (−O−*C*H_2−); 63.3 (−*C*H_2−OH); 43.8 (C, ox); 33.1, 29.9, 27.2, 26.4 (−*C*H_2−); 26.0 (CH_3−*C*H_2−); 8.6 (*C*H_3−).

3-Ethyl-3-(6-((4-vinylphenyl)methyl)oxyhexyl)-oxymethyloxetane C1. Sodium hydride (1.44 g, 60.0 mmol) was suspended in 130 mL of DMF under N_2 atmosphere. 3-Ethyl-3-(6-hydroxy-1-hexyl)oxyoxetane **1b** (10.8 g, 50.0 mmol) was added to the suspension. After being degassed and saturated with N_2, the mixture was stirred at 50 °C until the H_2 evolution had ceased (ca. 1 h). 4-Vinylbenzyl chloride (8.39 g, 55.0 mmol) was added, and the mixture was stirred at 90 °C for 16 h. After being cooled to room temperature, the solvent was removed in vacuo, and the residue was dissolved in 200 mL of diethyl ether and washed twice with 100 mL of water. The organic layer was dried over $MgSO_4$, and the solvent was evaporated. The crude product was purified by column chromatography (80 mm diameter, 25 cm length, silica gel, ethyl acetate/cyclohexane v/v 1.5:1) to give a clear, bright yellow liquid (10.8 g, 65%). $C_{21}H_{32}O_3$ (332.48 g/mol). Anal. Calcd (%): C, 75.86; H, 9.70. Found (%): C, 75.09; H, 9.51. ^{1}H NMR ($CDCl_3$) δ: 7.37 (d, 2H, $^3J_{H,H}$ = 8.01 Hz, H-phe); 7.27 (d, 2H, $^3J_{H,H}$ = 8.01 Hz, H-phe); 6.69 (dd, 1H, $^3J_{H,H}$ = 17.53 Hz, $^3J_{H,H}$ = 10.86 Hz, −C*H*=CH_2); 5.72 (dd, 1H, $^3J_{H,H}$ = 17.53 Hz, $^2J_{H,H}$ = 0.78 Hz, −CH=CH_2); 5.21 (dd, 1H, $^3J_{H,H}$ = 10.87 Hz, $^2J_{H,H}$ = 0.78 Hz, −CH=CH_2); 4.47 (s, 2H, −CH_2−O−); 4.42 (d, 2H, $^2J_{H,H}$ = 5.91 Hz, H-ox); 4.35 (d, 2H, $^2J_{H,H}$ = 5.91 Hz, H-ox); 3.50 (s, 2H, −O−CH_2−); 3.44 (t, 2H, $^3J_{H,H}$ = 6.66 Hz, −O−CH_2−); 3.42 (t, 2H, $^3J_{H,H}$ = 6.48 Hz, −CH_2−O−); 1.72 (q, 2H, $^3J_{H,H}$ = 7.44 Hz, −CH_2−CH_3); 1.58 (m, 4H, −CH_2−); 1.36 (m, 4H, −CH_2−); 0.86 (t, 3H, $^3J_{H,H}$ = 7.42 Hz, −CH_2−CH_3). ^{13}C NMR ($CDCl_3$) δ: 138.7, 137.3 (C, phe); 137.0 (C, vinyl); 128.2, 126.6, 114.0 (C, phe); 79.0 (-*C*H_2−, ox); 73.8, 73.0, 71.9,

70.7 ($-CH_2-O-$); 43.8 (C, ox); 30.1, 29.9, 27.1, 26.4, 26.4 ($-CH_2-$); 8.6 ($-CH_3$).

***tert*-Butyldimethylsilyl-(4-bromobenzyl) Ether.** 4-Bromobenzyl alcohol (9.35 g, 50.0 mmol) was dissolved in 120 mL of dichloromethane. After addition of *tert*-butyldimethylsilyl chloride (7.84 g, 52.0 mmol), the solution was chilled down to 0 °C. Then, pyridine (4.75 g, 60.0 mmol) was added dropwise within 15 min before stirring further for 10 min. After the ice bath was removed, the reaction mixture was stirred at room temperatur for 5 h. The mixture was washed twice each with 100 mL of 5% HCl_{aq} and dried over $MgSO_4$. After the solvent was removed in vacuo, the crude product was distilled at 140−150 °C/0.1 hPa in a glass oven to give a colorless liquid (14.5 g, 96%). $C_{13}H_{21}OSiBr$ (301.30 g/mol). Anal. Calcd (%): C, 51.82; H, 7.03; Si, 9.32; Br, 26.52. Found (%): C, 49.45; H, 6.57; Si, 8.65; Br, 26.76. ^{1}H NMR ($CDCl_3$) δ: 7.44 (dm, 2H, $^3J_{H,H} = 8.40$ Hz, H-phe o Br); 7.19 (dm, 2H, $^3J_{H,H} = 8.40$ Hz, H-phe m Br); 4.66 (s, 2H, phe−CH_2−O); 0.90 (s, 9H, −C(CH_3)$_3$); 0.10 (s, 6H, −Si(CH_3)$_2$−C). ^{13}C NMR ($CDCl_3$) δ: 140.8; 131.7; 128.1; 121.0; 64.7; 26.3; −3.5; −5.2.

***N,N*-Diphenyl-4-bromoaniline 2b**. Triphenylamine **2a** (29.4 g, 120 mmol) and NBS (21.4 g, 120 mmol) were dissolved in 500 mL of carbon tetrachloride. The solution was refluxed for 4 h. The precipitated succinimide was filtered, and the solvent was evaporated from the solution. The remaining gray oil was recrystallized from ethanol. The obtained white crystalline powder (36,2 g, 93%) was dried in a vacuum. $C_{18}H_{14}NBr$ (324.22 g/mol). Anal. Calcd (%): C, 66.68; H, 4.35; N, 4.42; Br, 24.64. Found (%): C, 66.63; H, 4.39; N, 4.36; Br, 24.27. ^{1}H NMR ($CDCl_3$) δ: 7.35−7.20 (m, 6H, H-ph m N, H-phe m N); 7.11−6.99 (m, 6H, H-ph o N, H-phe o N); 6.97−6.90 (m, 2H, H-ph p N). ^{13}C NMR ($CDCl_3$) δ: 147.4; 147.0; 132.1; 129.4; 125.1; 124.4; 123.2; 114.8.

General Procedure for the Synthesis of 4-(*N,N*-Diarylamino)-4′-bromobiphenyls 3b and 4b. Tris(dibenzylidene acetone) dipalladium(0) (192 mg, 0.210 mmol) and bis(diphenylphosphino) ferrocene (233 mg, 0.420 mmol) were dissolved under N_2 atmosphere in 250 mL of dry toluene. After being stirred for 10 min at room temperature to form the catalytic system, the diarylamine (**3a**, 5.08 g; **4a**, 6.58 g; 30.0 mmol) and 4,4′-dibromobiphenyl (31.2 g, 100.0 mmol) and sodium *tert*-butoxide (3.46 g, 36.0 mmol) were added to the solution. The mixture was degassed and saturated with N_2 before being stirred at 100 °C for 7 h. After being cooled to room temperature, the reaction mixture was diluted with 100 mL of toluene and washed twice with 150 mL of water. The toluene layer was dried over $MgSO_4$, and the solvent was removed in vacuo. The crude product was isolated by column chromatography (80 mm diameter, 25 cm length, silica gel) first with cyclohexane as eluent to recover the dibromobiphenyl then with toluene/cyclohexane v/v 1:1 to give the product as a white solid (**3b**, 8.2 g, 68%; **4b**, 10.5 g, 78%).

4-(*N,N*-Diphenylamino)-4′-bromobiphenyl 3b. $C_{24}H_{18}NBr$ (400.32 g/mol). Anal. Calcd (%): C, 72.01; H, 4.53; N, 3.50; Br, 19.96. Found (%): C, 72.39; H, 4.60; N, 3.61; Br, 19.52. ^{1}H NMR ($CDCl_3$) δ: 7.54−7.49 (m, 2H, H-dphe o Br); 7.44−7.34 (m, 4H, H-dphe); 7.30−7.21 (m, 4H, H-ph m N); 7.15−7.08 (m, 6H, H-ph o N, H-dphe o N); 7.07−7.00 (m, 2H, H-ph p N). ^{13}C NMR ($CDCl_3$) δ: 147.5; 139.6; 133.6; 131.8; 129.3; 128.2; 127.5; 124.6; 123.7; 123.1; 120.9.

4-(*N*-(1-Naphthyl)-*N*-phenylamino)-4′-bromobiphenyl 4b. $C_{28}H_{20}NBr$ (450.38 g/mol). Anal. Calcd (%): C, 74.67; H, 4.48; N, 3.11; Br, 17.74. Found (%): C, 75.02; H, 4.48; N, 3.24; Br, 17.43. ^{1}H NMR ($CDCl_3$) δ: 7.98−7.84 (m, 2H, H-na o/m N); 7.81−7.72 (m, 1H, H-na p N); 7.52−7.42 (m, 4H, H-dphe o Br, H-na); 7.41−7.28 (m, 6H, H-dphe, H-na); 7.25−7.13 (m, 2H, H-ph m N); 7.12−7.00 (m, 4H, H-ph o N, H-dphe o N); 7.00−6.92 (m, 1H, H-ph p N). ^{13}C NMR ($CDCl_3$) δ: 148.2; 148.0; 143.2; 139.6; 135.3; 132.6; 131.8; 131.2; 129.2; 128.4; 128.1; 127.4; 127.3; 126.7; 126.5; 126.4; 126.2; 124.2; 122.4; 122.2; 121.4; 120.7.

General Procedure for the Synthesis of *N,N,N′*-Triphenyl-*p*-phenylendiamine 2c and *N,N,N′*-Triarylbenzidines 3c, 4c, and 5c. Tris(dibenzylidene acetone) dipalladium(0) (91.6 mg, 0.100 mmol) and bis(diphenylphosphino) ferrocene (111 mg, 0,200 mmol) were dissolved under N_2 atmosphere in 150 mL of dry toluene. After being stirred for 10 min at room temperature to form the catalytic system, the bromoarene (**2b**, 6.48 g; **3b**, 8.01 g; **4b**, 9.01 g; 20.0 mmol), arylamine (aniline, 4.66 g; 1-naphthylamine, 7.16 g; 50.0 mmol), and sodium *tert*-butoxide (2.31 g, 24.0 mmol) were added to the solution. The solution was degassed and saturated with N_2 before being stirred at 100 °C for 6 h. After being cooled to room temperature, the reaction mixture was diluted with 100 mL of toluene and washed twice with 150 mL of water. The toluene layer was dried over $MgSO_4$, and the solution was concentrated to give a colored oil. The crude product was purified by column chromatography (80 mm diameter, 25 cm length, silica gel, toluene/cyclohexane, v/v 2:1) to give a clear, colored oil (**2c**) which crystallized after 2 days to a white or yellow solid (**2c**, 5.45 g, 81%; **3c**, 6.93 g, 84%; **4c**, 9.43 g, 92%; **5c**, 8.33 g, 90%;).

***N,N,N′*-Triphenyl-*p*-phenylenediamine 2c.** $C_{24}H_{20}N_2$ (336.44 g/mol). Anal. Calcd (%): C, 85.68; H, 5.99; N, 8.33. Found (%): C, 85.76; H, 5.99; N, 8.13. ^{1}H NMR ($CDCl_3$) δ: 7.28−7.21 (m, 6H, H-ph m N); 7.12−7.05 (m, 6H, H-ph o N); 7.03−6.92 (m, 7H, H-ph p N, H-phe). ^{13}C NMR ($CDCl_3$) δ: 147.9; 143.1; 141.2; 137.6; 129.9; 129.4; 123.1; 122.4; 121.6; 118.9; 118.0; 117.9.

***N,N,N′*-Triphenylbenzidine 3c.** $C_{30}H_{24}N_2$ (412.54 g/mol). Anal. Calcd (%): C, 87.34; H, 5.86; N, 6.79. Found (%): C, 87.26; H, 5.98; N, 6.60. ^{1}H NMR ($CDCl_3$) δ: 7.47−7.36 (m, 4H, H-dphe m N); 7.30−7.20 (m, 6H, H-ph m N); 7.16−7.04 (m, 10H, H-ph o N, H-dphe o N); 7.04−6.96 (m, 3H, H-ph p N). ^{13}C NMR ($CDCl_3$) δ: 149.2; 147.6; 145.0; 144.2; 136.6; 133.4; 130.3; 130.1; 128.2; 128.0; 125.6; 125.2; 123.7; 121.2; 118.5; 118.4.

***N*-Phenyl-*N,N′*-dinaphthylbenzidine 4c.** $C_{38}H_{28}N_2$ (512.66 g/mol). Anal. Calcd (%): C, 89.03; H, 5.51; N, 5.46. Found (%): C, 89.13; H, 5.59; N, 5.02. ^{1}H NMR ($CDCl_3$) δ: 8.05−7.84 (m, 4H, H-na o/m N); 7.78−7.73 (m, 1H, H-na p N); 7.59−7.56 (m, 1H, H-na p N); 7.51−7.32 (m, 8H, H-na); 7.27−7.15 (m, 6H, H-ph m N, H-dphe m N); 7.06−7.00 (m, 6H, H-ph o N, H-dphe o N); 6.95−6.90 (m, 1H, H-ph p N); 2.35 (s, 1H, N−*H*). ^{13}C NMR ($CDCl_3$) δ: 148.4; 147.4; 147.2; 143.5; 135.3; 134.7; 134.0; 134.5; 134.4; 131.3; 129.1; 129.0; 128.6; 128.4; 128.2; 127.6; 127.4; 127.3; 127.1; 126.5; 126.4; 126.3; 126.2 126.1; 126.0; 125.8; 125.3; 124.3; 122.0; 121.9; 121.8; 121.7; 117.9; 116.4.

***N,N′*-Diphenyl-*N*-naphthylbenzidine 5c.** $C_{34}H_{26}N_2$ (462.60 g/mol). Anal. Calcd (%): C, 88.28; H, 5.67; N, 6.06. Found (%): C, 88.57; H, 5.75; N, 5.81. ^{1}H NMR ($CDCl_3$) δ: 8.04−7.82 (m, 2H, H-na o/m N); 7.59−7.56 (m, 1H, H-na p N); 7.53−7.47 (m, 4H, H-na); 7.47−7.36 (m, 4H, H-dphe m N); 7.30−7.20 (m, 4H, H-ph m N); 7.16−7.04 (m, 8H, H-ph o N, H-dphe o N); 7.04−6.96 (m, 2H, H-ph p N). ^{13}C NMR ($CDCl_3$) δ: 149.2; 147.6; 145.0; 144.2; 136.6; 133.4; 130.3; 130.1; 128.2; 128.0; 125.6; 125.2; 123.7; 121.2; 118.5; 118.4.

General Procedure for the Synthesis of *N,N,N′*-Triphenyl-*N′*-(4-(hydroxymethyl)phenyl)-*p*-phenylenediamine 2d and *N,N,N′*-Triaryl-*N′*-(4-(hydroxymethyl)-phenyl)benzidines 3d, 4d, and 5d. *1. C−N coupling.* Tris(dibenzylidene acetone) dipalladium(0) (91.6 mg, 0,100 mmol) and tri-*tert*-butylphosphane (122 mg, 0.600 mmol) were dissolved under N_2 in 130 mL of dry toluene. After being stirred for 10 min at room temperature to form the catalytic system, the arylamine, (**2c**, 6.73 g; **3c**, 8.25 g; **4c**, 10.25 g; **5c**, 9.25 g; 20.0 mmol), *tert*-butyldimethylsilyl-(4-bromobenzyl) ether (6.03 g, 20.0 mmol) and sodium *tert*-butoxide (2.31 g, 24.0 mmol) were added to the solution. The solution was degassed and saturated with N_2 before being stirred at 100 °C for 5 h. After being cooled to RT, the reaction mixture was diluted with 100 mL of toluene and washed with 200 mL of a saturated solution of sodium chloride. The organic phase was dried over $MgSO_4$, and the solvent was evaporated to give a colored solid.

2. Deprotection. The product of the first synthetic step was dissolved in 200 mL of THF. After the addition of 21.0 mL of tetra-*n*-butylammonium fluoride solution (1.0 mol/L, contains 5% water), the solution was stirred for 2 h at RT. The solvent was removed, and the product was purified by column chro-

matography (80 mm diameter, 25 cm length, silica gel, toluene/ethyl acetate 2:1) to yield a weakly colored solid (**2d**, 7.26 g, 82%; **3d**, 8.82 g, 85%; **4d**, 11.0 g, 89%; **5d**, 10.12 g, 89%).

***N,N,N′*-Triphenyl-*N′*-(4-(hydroxymethyl)phenyl)-*p*-phenylene-diamine 2d.** $C_{31}H_{26}ON_2$ (442.56 g/mol). El. Anal. Calcul. (%): C 84.13; H 5.92; N 6.33. found (%): C 83.79; H 5.87; N 6.17. ^{1}H NMR ($CDCl_3$) δ 7.27−7.20 (m, 8H, H-ph m N); 7.11−7.05 (m, 8H, H-ph o N); 7.01−6.92 (m, 7H, H-ph p N, H-phe). ^{13}C NMR ($CDCl_3$) δ 147.8; 147.5; 143.0, 142.7; 134.7; 129.2; 128.3; 125.5; 125.4; 123.8; 123.6; 122.5; 122.4; 65.1. EI-MS *m/z* (%): 441.8 ($M^{+\bullet}$, 100); 220.9 (M^{2+}, 19).

***N,N,N′*-triphenyl-*N′*-(4-(hydroxymethyl)phenyl)benzidine 3d.** $C_{37}H_{30}ON_2$ (518.70 g/mol). Anal. Calcd (%): C, 85.68; H, 5.83; N, 5.40. Found (%): C, 85.15; H, 6.00; N, 5.13. ^{1}H NMR ($CDCl_3$) δ: 7.47−7.35 (m, 4H, H-dphe m N); 7.29−7.19 (m, 8H, H-ph m N); 7.15−7.05 (m, 12H, H-dphe o N, H-ph o N); 7.04−6.96 (m, 3H, H-ph p N). ^{13}C NMR ($CDCl_3$) δ: 147.7; 147.6; 147.3; 146.8; 146.6; 135.2; 134.9; 134.7; 129.3; 129.2; 128.3; 127.3; 124.4; 124.3; 124.2; 124.0; 123.0; 122.8; 65.1. *m/z* (%): 517.9 ($M^{+\bullet}$, 100); 258.9 (M^{2+}, 30).

***N,N′*-Dinaphthyl-*N*-phenyl-*N′*-(4-(hydroxymethyl)phenyl)benzidine 4d.** $C_{45}H_{34}ON_2$ (618.78 g/mol). Anal. Calcd (%): C, 87.35; H, 5.54; N, 4.53. Found (%): C, 86.86; H, 5.79; N, 4.05. ^{1}H NMR ($CDCl_3$) δ: 7.97−7.81 (m, 4H, H-na o/m N); 7.79−7.70 (m, 2H, H-na p N); 7.50−7.26 (m, 12H, H-dphe m N, H-na); 7.25−7.12 (m, 4H, H-ph m N, H-bz m N); 7.09−6.97 (m, 8H, H-ph o N, H-dphe o N, H-bz o N); 6.96−6.89 (m, 1H, H-ph p N); 4,59 (s, 2H, phe−CH_2−OH). ^{13}C NMR ($CDCl_3$) δ: 148.3; 148.0; 147.3; 147.1; 143.5; 143.3; 135.3; 134.1; 134.0; 133.8; 131.3; 131.2; 129.1; 129.0; 128.4; 128.3; 127.2; 127.1; 126.6; 126.5; 126.4; 126.3; 126.2, 126.1; 125.3; 124.3; 124.2; 122.1; 122.0; 121.9; 121.8; 65.2. EI-MS *m/z* (%): 617.9 ($M^{+\bullet}$, 100); 309.0 (M^{2+}, 14).

***N*-Naphthyl-*N,N′*-diphenyl-*N′*-(4-(hydroxymethyl)phenyl)benzidine 5d.** $C_{41}H_{32}ON_2$ (568.72 g/mol). Anal. Calcd (%): C, 86.59; H, 5.67; N, 4.93. Found (%): C, 86.30; H, 5.66; N, 4.46. ^{1}H NMR ($CDCl_3$) δ: 7.98−7.84 (m, 2H, H-na o/m N); 7.79−7.74 (m, 1H, H-na p N); 7.50−7.28 (m, 8H, H-dphe m N, H-na); 7.28−7.13 (m, 6H, H-ph m N, H-bz m N); 7.13−7.02 (m, 10H, H-ph o N, H-dphe o N, H-bz o N); 7.02−6.90 (m, 2H, H-ph p N); 4.59 (s, 2H, phe−CH_2−OH). ^{13}C NMR ($CDCl_3$) δ: 148.3; 147.7; 147.4; 147.3; 146.5; 143.4; 137.0; 135.3; 134.9; 133.7; 131.3; 129.4; 129.1; 128.4; 128.2; 128.0; 127.3; 127.2; 126.5; 126.4; 126.3; 126.2; 124.3; 124.2; 124.0; 122.8; 122.0; 121.8; 71.9. EI-MS *m/z* (%): 567.9 ($M^{+\bullet}$, 100); 284.0 (M^{2+}, 14).

General Procedure for Synthesis of the Monomers H2, H3, H4, and H5. The hydroxymethyl-substituted arylamine (**2d**, 4.43 g; **3d**, 5.19 g; **4d**, 6.19 g; **5d**, 5.69 g; 10.0 mmol) was dissolved in 100 mL of dry toluene under N_2 atmosphere. After addition of potassium (430 mg, 11.0 mmol), the reaction mixture was stirred vigorously at 100 °C until the potassium had dissolved completely and the H_2 evolution had ceased (about 3 h). 4-Vinylbenzyl chloride (1.83 g, 12.0 mmol) was given to the cloudy suspension, which was then stirred at 90 °C for 20 h. The solution was diluted with 70 mL of toluene and then washed with 150 mL of a saturated NaCl solution. After evaporation of the solvent, the product was isolated by column chromatography (80 mm diameter, 20 cm length, silica gel, toluene/cyclohexane 3:1) to give a colorless glass. After being freeze-dryed, a colorless product was yielded (**H2**, 3.30 g, 59%; **H3**, 3.49 g, 55%; **H4**, 4.41 g, 60%; **H5**, 4.18 g, 61%).

***N,N,N′*-Triphenyl-*N′*-(4-((4-vinylphenyl)methoxymethyl)phenyl)-*p*-phenylenediamine H2.** $C_{40}H_{34}ON_2$ (558.73 g/mol). Anal. Calcd (%): C, 85.99; H, 6.13; N, 5.01. Found (%): C, 85.63; H, 6.34; N, 4.79. ^{1}H NMR ($CDCl_3$) δ: 7.40−6.95 (m, 27H, H-arom); 6.73 (dd, 1H, $^3J_{HH}$ = 10.86 Hz, $^3J_{HH}$ = 17.73 Hz, ph−CH=CH_2); 5.76 (d, 1H, $^3J_{HH}$ = 17.73 Hz, ph−CH=CH_2); 5.24 (d, 1H, $^3J_{HH}$ = 10.86 Hz, ph−CH=CH_2); 4.55 (s, 4H, −O−CH_2−). ^{13}C NMR ($CDCl_3$) δ: 141.6; 140.7; 136.4; 136.0; 135.8; 134.0; 131.6; 129.4; 128.5; 127.5; 126.1; 122.9; 122.4; 112.3; 69.4; 66.0. EI-MS *m/z* (%): 558.4 ($M^{+\bullet}$, 100); 425.2 (63).

***N,N,N′*-Triphenyl,*N′*-(4-((4-vinylphenyl)methoxymethyl)phenyl)benzidine H3.** $C_{46}H_{38}ON_2$ (634.82 g/mol). Anal. Calcd (%): C, 87.03; H, 6.03; N, 4.41. Found (%): C, 87.10; H, 5.86; N, 4.09. ^{1}H NMR ($CDCl_3$) δ: 7.47−7.29 (m, 8H, H-phe m N, H-vbz); 7,28−7,17 (m, 8H, H-ph m N, H-dphe m N); 7.15−7.05 (m, 12H, H-dphe o N, H-ph o N); 7.05−6.97 (m, 3H, H-ph p N); 6.71 (dd, 1H, $^3J_{HH}$ = 10,86 Hz, $^3J_{HH}$ = 17,56 Hz, ph−CH=CH_2); 5.74 (d, 1H, $^3J_{HH}$ = 17,56 Hz, ph−CH=CH_2); 5.23 (d, 1H, $^3J_{HH}$ = 10.86 Hz, ph−CH=CH_2); 4.57/4.48 (s/s, 4H, −O−CH_2−). ^{13}C NMR ($CDCl_3$) δ: 147.7; 147.6; 147.3; 146.8; 146.6; 137.9; 137.0; 136.6; 134.8; 134.7; 132.5; 129.2; 129.1; 128.0; 127.3; 126.3; 124.3; 124.1; 124.0; 122.9; 122.8; 113.8; 71.9; 71.8. EI-MS *m/z* (%): 634.4 ($M^{+\bullet}$, 100); 501.2 (65).

***N,N′*-Dinaphthyl-*N*-phenyl-*N′*-(4-((4-vinylphenyl)-methoxymethyl)phenyl)benzidine H4.** $C_{54}H_{42}ON_2$ (734,94 g/mol). Anal. Calcd (%): C, 88.25; H, 5.76; N, 3.81. Found (%): C, 88.02; H, 5.76; N, 3.49. ^{1}H NMR ($CDCl_3$) δ: 7.97−7.81 (m, 4H, H-na o/m N); 7.79−7.70 (m, 2H, H-na p N); 7.50−7.26 (m, 16H, H-dphe m N, H-na, H-vbz); 7.25−7.10 (m, 4H, H-ph m N, H-dphe m N); 7.09−6.97 (m, 8H, H-ph o N, H-dphe o N); 6.96−6.89 (m, 1H, H-ph p N); 6.71 (dd, 1H, $^3J_{HH}$ = 10,89 Hz, $^3J_{HH}$ = 17,74 Hz, ph−CH=CH_2); 5.74 (d, 1H, $^3J_{HH}$ = 17.74 Hz, ph−CH=CH_2); 5.23 (d, 1H, $^3J_{HH}$ = 10.89 Hz, ph−CH=CH_2); 4.54/4.45 (s/s, 4H, −O−CH_2−). ^{13}C NMR ($CDCl_3$) δ: 148.3; 147.9; 147.3; 147.2; 145.6; 143.4; 138.0; 137.0; 136.6; 135.3; 133.9; 133.8; 131.4; 131.3; 131.2; 129.1; 129.0; 128.4; 128.2; 128.0; 127.2; 127.1; 126.5−126.3; 126.2; 126.1; 125.3; 124.3; 122.0; 121.9; 121.7; 113.7; 71.8. EI-MS *m/z* (%): 734.1 ($M^{+\bullet}$, 100); 600.9 (38); 366.9 (M^{2+}, 9).

***N*-Naphthyl,*N,N′*-diphenyl-*N′*-(4-((4-vinylphenyl)-methoxymethyl)phenyl)benzidine H5.** $C_{50}H_{40}ON_2$ (684.88 g/mol). Anal. Calcd (%): C, 87.69; H, 5.89; N, 4.09. Found (%): C, 88.01; H, 5.84; N, 3.85. ^{1}H NMR ($CDCl_3$) δ: 7.98−7.84 (m, 2H, H-na o/m N); 7.79−7.74 (m, 1H, H-na p N); 7.50−7.28 (m, 12H, H-dphe m N, H-vbz, H-na); 7.28−7.13 (m, 6H, H-ph m N, H-bz m N); 7.13−7.02 (m, 10H, H-ph o N, H-dphe o N, H-bz o N); 7.02−6.90 (m, 2H, H-ph p N); 6.71 (dd, 1H, $^3J_{HH}$ = 10.87 Hz, $^3J_{HH}$ = 17.73 Hz, ph−CH=CH_2); 5.73 (d, 1H, $^3J_{HH}$ = 17.73 Hz, ph−CH=CH_2); 5.22 (d, 1H, $^3J_{HH}$ = 10.87 Hz, ph−CH=CH_2); 4.57/4.48 (s/s, 4H, −CH_2−O−). ^{13}C NMR ($CDCl_3$) δ: 148.3; 147.7; 147.4; 147.3; 146.5; 143.4; 137.9; 137.0; 136.6; 135.3; 134.9; 133.7; 132.5; 131.2; 129.2; 129.1; 129.0; 128.4; 128.2; 128.0; 127.3; 127.2; 126.5; 126.4; 126.3; 126.2; 126.1; 124.3; 124.2; 124.0; 122.8; 122.0; 121.8; 113.8; 71.9; 71.8. EI-MS *m/z* (%): 683.9 ($M^{+\bullet}$, 100); 540.9 (40); 341.9 (M^{2+}, 6).

Synthesis of Polymers P1A/B−P4A/B. The procedure described for **P1A** is generally applicable to all other polymerizations. **C1** (332 mg, 1.00 mmol) and **H2** (559 mg, 1.00 mmol) were dissolved in 4 mL of toluene. After degassing of the mixture and saturation with N_2, α,α′-azo-bis(isobutyronitrile) (4.00 mg, 2 mg/mmol monomer) was added and the solution was stirred 24 h at 80 °C. The mixture was diluted with 3 mL of toluene, and the polymer was precipitated by rapid injection of the solution into 200 mL of methanol. The polymer was collected by filtration and dried in vacuo to yield a white solid (820 mg, 92%). The crude polymer was redissolved in 6 mL of $CHCl_3$ and precipitated again as described above before using it for the experiments and analytics. Anal. Calcd **P1A** (%): C, 82.2; H, 7.5; N, 3.1. Found (%): C, 82.0; H, 7.4; N, 3.1. Anal. Calcd **P1B** (%): C, 84.3; H, 5.1; N, 4.2. Found (%): C, 84.3; H, 5.7; N, 4.1. Anal. Calcd **P2A** (%): C, 83.2; H, 7.3; N, 2.9. Found (%): C, 83.3; H, 7.1; N, 2.9. Anal. Calcd **P2B** (%): C, 85.4; H, 6.6; N, 3.8. Found (%): C, 89.1; H, 6.6; N, 3.8. Anal. Calcd **P3A** (%): C, 84.4; H, 7.0; N, 2.6. Found (%): C, 84.9; H, 6.5; N, 2.6. Anal. Calcd **P3B** (%): C, 86.6; H, 6.3; N, 3.3. Found (%): C, 86.1; H, 6.2; N, 3.1. Anal. Calcd **P4A** (%): C, 83.8; H, 7.1; N, 2.8. Found (%): C, 84.0; H, 6.7; N, 2.7. Anal. Calcd **P4B** (%): C, 86.0; H, 6.4; N, 3.5. Found (%): C, 85.9; H, 6.1; N, 3.5.

Cross-Linking Procedure. Commercially available microscope glass slides were used as the substrates. They were carefully cleaned and dried before use. Solutions of the polymers **P1A/B−P4A/B** in tetrahydrofuran/toluene(v/v = 1:1) solution were prepared, and varying amounts of the photoinitiator **6** were added shortly before spincoating, yielding films of about 100-nm thickness. After spin-coating, the films were irradiated with a UV lamp (λ = 365 nm) for 10 s. To promote cross-linking, the films were cured at temperatures varying

from 25 °C (room temperature) to 150 °C for 1 min, respectively. A UV−vis spectrum of the film was taken. To test the solvent resistivity of the material, the film was then exposed to THF, which is an excellent solvent for all polymers studied here. We found that by simply rinsing the film with THF, similar results as immersing the film into a THF bath with applied ultrasound could be obtained. After this, another UV−vis spectrum was recorded. The film resistivity was then defined as the ratio of the peak absorption after and before THF treatment. All steps were performed in inert gas atmosphere and under red-light conditions.

Electrochemical Measurements. Cyclic voltammetry (CV) was processed on a Gamry PC4/300 PC built-in potentiostat with a three-electrode cell in a solution of Bu_4NBF_4 (0.05 M) in acetonitrile at scan rates of 10−100 mV/s. The polymer films were coated onto the working electrode, a Pt wire of 1 mm diameter with a length of 10 mm, by dipping the electrode into a solution of the polymer (20 g/L) and the photoinitiator (1 mol% relating to oxetane groups) in THF. After drying in air, the film was cross-linked by UV irradiation (10 s) with a mercury low-pressure fluorescent lamp (λ_{max} = 366 nm) and tempering in air at 120 °C for 1 min. A Pt plate of 100 mm^2 was used as the counter electrode. A silver wire coated with AgCl was used to form the reference electrode. Ferrocene was used as a reference substance and was measured by dissolving it in the acetonitrile-based solution.

Device Preparation. ITO(indium tin oxide)-coated glass substrates were commercially obtained from Merck display glass (20 Ω/$in.^2$) and carefully cleaned and dried before use. The ITO was treated by an ozone plasma, which alters the work function to about 5.4 eV. Hole-only devices were obtained following the film deposition procedure outlined above. The initiator content was 1 wt%, and the curing was performed at 150 °C for 1 min. The films were then rinsed with THF to remove the soluble decomposition products of the PI, as well as non-cross-linked material (e.g., decomposition products of the PI). Finally, Ag (150 nm) is deposited by thermal vacuum evaporator as the top electrode. The entire characterization was performed in a glovebox under inert gas atmosphere.

Acknowledgment. Financial support provided by the Bundesministerium für Bildung und Forschung (BMBF) through Project No. 13N8214, the Deutsche Forschungsgemeinschaft (DFG), and the Bavarian government (Promotionsstipendium for E.B.) is gratefully acknowledged. We thank B. Lerche, L. Friebe, J. Krause, and M. Barth (all TU München) for technical support.

References and Notes

(1) Tak, Y. H.; Vestweber, H.; Bässler, H.; Bleyer, A.; Stockmann, R.; Hörhold, H.-H. *Chem. Phys.* **1996**, *212*, 471−485.

(2) Allen, N. S.; Khan, L.; Edge, M.; Billings, M.; Veres, J. *J. Photochem. Photobiol., A* **1998**, *116*, 235−244.

(3) Yoshimoto, N.; Hanna, J.-I. *J. Mater. Chem.* **2003**, *13*, 1004−1010.

(4) Bozano, L. D.; Carter, K. R.; Lee, V. Y.; Miller, R. D.; DiPietro, R.; Scott, J. C. *J. Appl. Phys.* **2003**, *94*, 3061−3068.

(5) Contoret, A. E. A.; Farrar, S. R.; Khan, S. M.; O'Neill, M.; Richards, G. J.; Aldred, M. P.; Kelly, S. M. *J. Appl. Phys.* **2003**, *93*, 1465−1467.

(6) Yoshimoto, N.; Hanna, J.-I. *Adv. Mater.* **2002**, *14*, 988−991.

(7) Zhang, Y.-D.; Hreha, R. D.; Jabbour, G. E.; Kippelen, B.; Peyghambarian, N.; Marder, S. R. *J. Mater. Chem.* **2002**, *12*, 1703−1708.

(8) Le Barny, P.; Bouche, C.-M.; Facoetti, H.; Soyer, F.; Robin, P. *Proc. SPIE-Int. Soc. Opt. Eng.* **1997**, *3148*, 160−169.

(9) Domercq, B.; Hreha, R. D.; Zhang, Y.-D.; Larribeau, N.; Haddock, J. N.; Schultz, C.; Marder, S. R.; Kippelen, B. *Chem. Mater.* **2003**, *15*, 1491−1496.

(10) Nuyken, O.; Böhner, R.; Erdmann, C. *Macromol. Symp.* **1996**, *107*, 125−138.

(11) Braig, T.; Bayerl, M. S.; Nuyken, O.; Müller, D. C.; Gross, M.; Meerholz, K. *Polym. Mater. Sci. Eng.* **1999**, *80*, 122−123.

(12) Braig, T.; Müller, D. C.; Gross, M.; Meerholz, K.; Nuyken, O. *Macromol. Rapid Commun.* **2000**, *21*, 583−589.

(13) Bayerl, M. S.; Braig, T.; Nuyken, O.; Müller, D. C.; Gross, M.; Meerholz, K. *Macromol. Rapid Commun.* **1999**, *20*, 224−228.

(14) Campbell, T. W. *J. Org. Chem.* **1957**, *22*, 1029.

(15) Bodenbrenner, K.; Wegler, R. (Farbenfabrik Bayer AG), DE 1 021 858, 1960, *Chem. Abstr.* 1960; Vol. 54, p 4617.

(16) Guram, A. S.; Rennels, R. A.; Buchwald, S. L. *Angew. Chem., Int. Ed. Engl.* **1995**, *34*, 1348−1350.

(17) Louie, J.; Hartwig, J. F. *Tetrahedron Lett.* **1995**, *36*, 3609−3612.

(18) Yamamoto, T.; Nishiyama, M.; Koie, Y. *Tetrahedron Lett.* **1998**, *39*, 2367−2370.

(19) Sasaki, H.; Crivello, J. V. *J. Macromol. Sci., Pure Appl. Chem.* **1992**, *A29*, 915−930.

(20) Fouassier, J.-P. *Photoinitiation, Photopolymerization and Photocuring: Fundamentals and Application*; Hanser Publishers: Munich, Vienna, New York, Cincinnati, 1995.

(21) Coropceanu, V.; Gruhn, N. E.; Barlow, S.; Lambert, C.; Durivage, J. C.; Bill, T. G.; Noell, G.; Marder, S. R.; Bredas, J.-L. *J. Am. Chem. Soc.* **2004**, *126*, 2727−2731.

(22) Nuyken, O.; Bacher, E.; Braig, T.; Faber, R.; Mielke, F.; Rojahn, M.; Wiederhirn, V.; Meerholz, K.; Müller, D. *Des. Monom. Polym.* **2002**, *5*, 195−210.

(23) Rojahn, M. Ph.D. Thesis, Technische Universität München, 2003.

(24) Schneider, M.; Hagen, J.; Haarer, D.; Müllen, K. *Adv. Mater.* **2000**, *12*, 351.

MA048365H